Theoretical Analysis of Isolated Bidirectional Dual Full Bridge ZVS DC-DC Converter with Novel Triple Phase-shift Control

Kuiyuan Wu[1] William G.Dunford[1] Clarence W.de Silva[2]

Abstract-This paper analyzes the working theory of the bidirectional dual full bridge ZVS DC-DC converter with novel triple-phase-shift control. This novel control method makes the efficiency and output voltage stability of the bidirectional converter more robust (insensitive) to parameter and output power change. Based on its working theory, the converter is separated into several stages. Detailed operation in each stage is analyzed. Equivalent circuits and necessary equations are built for each stage. Then, the ratio of the output voltage and input voltage, average input active power, average output active power and efficiency are solved theoretically in this paper. Relevant simulation results are attached in this paper. The forward and backward efficiency of this bidirectional converter with novel triple-phase-shift control are very high in large load scope.

Keywords-Isolated bidirectional ZVS DC-DC converter, novel triple-phase-shift control method, equivalent circuit, periodical operation, robust (insensitive) efficiency to parameter or output power change, high efficiency in large load scope.

I. Introduction

In recent years, the development of high power and large power range isolated bidirectional dc-dc converters has become an important topic because of the requirements of electric automobile, energy storage systems and aviation power system [2], [4], [8], [13]. This project is to design a forward $1kW/200V(93\%)$ and backward $250W/48V(95\%)$ bidirectional converter. The dual active full bridge converter is symmetry in both sides of the isolation transformer. It is suitable to be used as the power circuit to transfer energy back and forth, especially for high power case [12], [14], [17]. Therefore, it is used as the power circuit for this project. There are two series inductors $L01$ and $L02$ in Fig. 1. These two inductors are mainly used to enlarge ZVS scope, eliminate the switching loss and ensure the converter have high efficiency in large load scope [1], [5], [11], [18].

There are several existing control methods for this power circuit, like single phase-shift control [3], dual phase-shift control [4]. However, the novel triple phase-shift control method will make the system with high efficiency (Higher than 97%) in large load scope, especially when parameter changes. It is very important to make the efficiency of the bidirectional converter more robust (insensitive) to parameter change and different output power because this will make the converter more suitable for different applications. This approach does not appear to have been published until now in this area.

The paper first received 31 October 2017 and in revised form 20 Jun 2018. Digital Ref: APEJ-2017-10-0521

[1]**Department of Electrical and Computer Engineering, The University of British Columbia, Vancouver, BC, V6T 1Z4, Canada,**

[2]**Department of Mechanical Engineering, The University of British Columbia, Vancouver, BC, V6T 1Z4, Canada,**

(Email: wukuiyuan2010@hotmail.com)

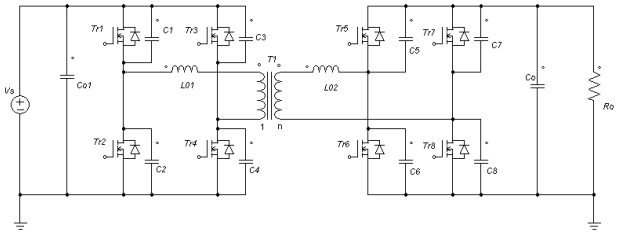

Fig. 1: The power circuit of the bidirectional converter

In novel triple-phase-shift control method, three control variables cooperate together to transfer energy. This will make the efficiency of the bidirectional DC-DC converter more robust (insensitive) to parameter change and different output powers. This project is simulated with PSIM software. Novel triple phase-shift control method is described in detail in Section II; the operation of bidirectional dual full bridge converter with novel triple phase-shift control is analyzed and equivalent circuits are derived in Section III; important equations of this bidirectional converter with novel triple phase-shift control are determined in Section IV; voltage ratio, active power and efficiency expressions of this bidirectional converter with triple phase-shift control are solved in Section V; the results obtained from theoretical analysis are validated by simulations and discussed in Section VI; finally, the main contributions of this paper are summarized in Section VII.

II. Novel Triple-Phase-Shift Control Method For Dual Active Full Bridge Converter

A. Brief Statement of this Method

This novel triple-phase-shift control method described in this paper is neither the same as common phase-shift methods in which all control signals are half duty cycle nor the same as common single phase-shift plus PWM control method in which the duty cycle of control signals can vary from zero to one [9]. In this method, four control signals $(Vg1, Vg2, Vg5, Vg6)$ with half duty cycle; another two control signals $(Vg3, Vg4)$ with duty cycle varying between zero and 50%; the last two control signals $(Vg7, Vg8)$ with another duty cycle varying between zero and 50%. This will make the controller easier to be realized with lead-lag compensator [6], [7]. Because the work theory of this new method is similar to that of common triple-phase-shift control method, it is called novel triple-phase-shift control method in this paper. This can be seen clearly in the following simulation results and work theory analysis.

In this novel triple-phase-shift controller, the first phase-shift between the primary control signal and the corresponding secondary control signal $(Vg1\ and\ Vg5)$, the second phase-shift between the diagonal control signals in the primary power circuit $(Vg1\ and\ Vg4)$ and the third phase-shift between the diagonal control signals in the secondary power circuit $(Vg5\ and\ Vg8)$ cooperate together to control energy transfer of the bidirectional DC-DC converter.

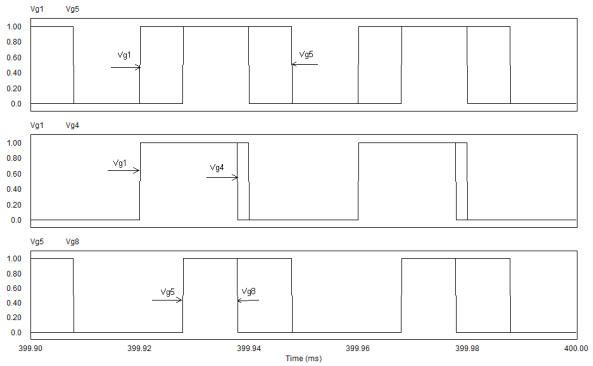

Fig. 2: Novel Triple-Phase-shift Control Signal Waveforms

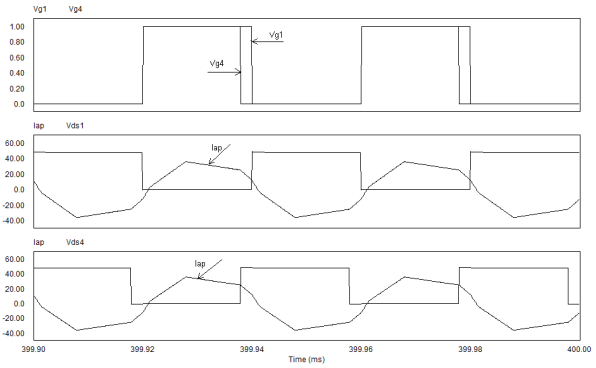

Fig. 3: Forward Control Signals, Power Switch Voltages and Primary Current with Novel Triple-Phase-shift Control

Corresponding control signal wave forms can be seen clearly in Fig. 2.

B. Forward Simulation Results of Control Signals, Power Switch Voltages and Primary Current

From Fig. 3, it can be found that the primary power circuit can realize ZVS very well because the primary current is negative when MOSFET1 and MOSFET4 turn on. This means the primary current passed through anti-parallel diodes $D1$ and $D4$ just before the power MOSFETs turn on; ZVS can be realized very well.

From Fig. 4, it can be found that the secondary power circuit can realize ZVS very well because the secondary current is positive when

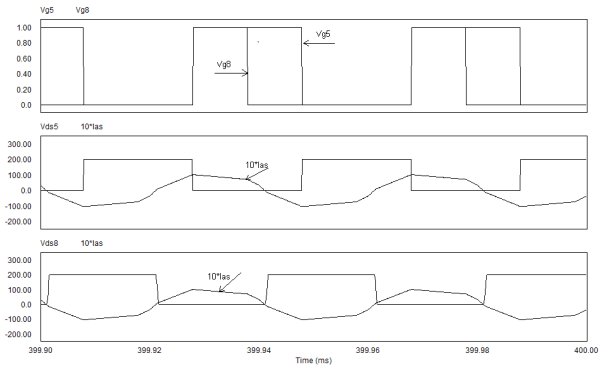

Fig. 4: Forward Control Signals, Power Switch Voltages and Secondary Current with Novel Triple-Phase-shift Control

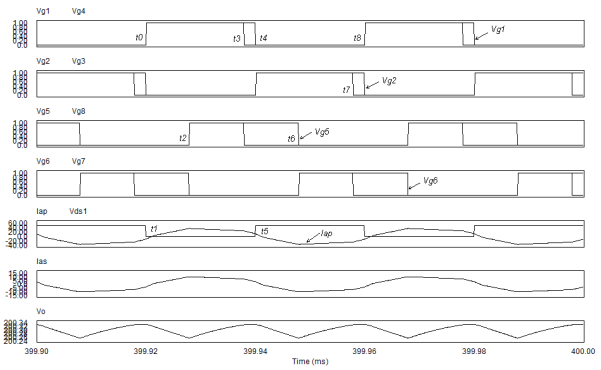

Fig. 5: Simulation Wave Forms of the Forward Bidirectional Converter with Novel Triple-Phase-shift Control for Vref1=6V

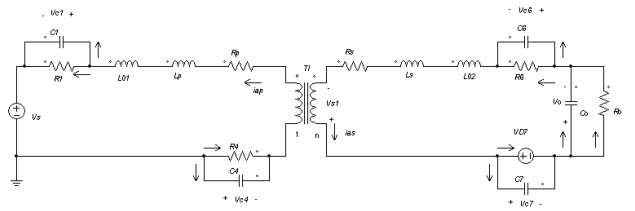

Fig. 6: Equivalent Circuit in Stage 1

MOSFET5 and MOSFET8 turn on. From the positive direction of secondary current in Fig. 1, it can be found that positive secondary current means it passed through anti-parallel diodes $D5$ and $D8$ just before the power MOSFETs turn on; ZVS can be realized very well, too. Therefore, the switching loss of this converter is eliminated [16]. For high frequency converter, switching loss is an important factor to influence efficiency [15].

III. Operation And Equivalent Circuit Of Forward Bioirectional Dual Full Bridge Converted With Novel Triple-Phase-Shift Control

The forward simulation wave-forms of bidirectional dual full bridge converter with novel triple phase-shift control are as follows.

Based Fig. 5, the forward bidirectional converter can be separated into eight stages. Corresponding equivalent circuits and necessary equations can be got in each stage. The backward converter can be analyzed similarly.

1: Stage 1 $t_0 - t_1$: Power switches $Tr1$ and $Tr4$ will turn on at $t = t_0$. Because the primary current is still negative during this period, the primary current will flow through $Tr4/Tr1$ and the inductor energy flows back to the power source.

Because $Vg5/Vg8/Vg7$ are equal to zero, $Tr5/Tr8/Tr7$ all in Off state; $Vg6 = 1$, $Tr6$ is On. $I_{as} < 0$, secondary current flows through $Tr6/D7$. The inductor $L02$ and output capacitor provide energy to the load. The output voltage reduces during this period. The equivalent circuit in this stage is Fig. 6:

2: Stage 2 $t_1 - t_2$: Because $Vg1/Vg4 = 1$, power switches $Tr1$ and $Tr4$ are in On state in this period. Because the primary current is positive during this period, the primary current will flow through $Tr1/Tr4$ and the inductor $L01$ and transformer leakage inductance. The energy will transfer from the primary side to the secondary side.

Because $Vg5/Vg8/Vg7$ are equal to zero, $Tr5/Tr8/Tr7$ all in Off state; $Vg6 = 1$, $Tr6$ is On. $I_{as>0}$, secondary current will charge

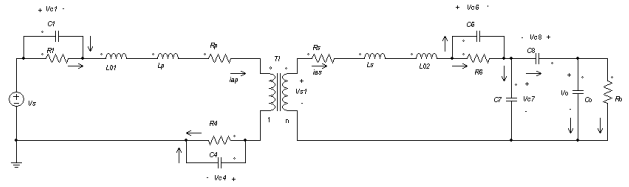

Fig. 7: C8 Discharging Equivalent Circuit in Stage 2

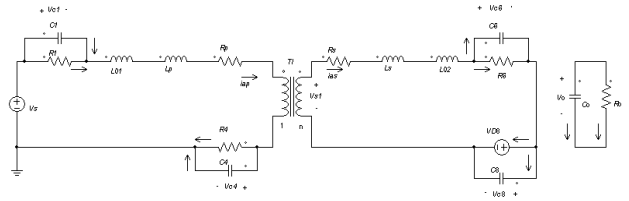

Fig. 8: Free Wheeling Equivalent Circuit in Stage 2

capacitor $C7$ and discharge capacitor $C8$ till its voltage reduces to the forward conduction voltage of diode $D8$. The equivalent circuit is Fig. 7.

Then the current flows through $Tr6/D8$. The energy is stored in the secondary inductor $L02$ and leakage inductor because this is a freewheeling period with no power transfer to the load theoretically. Output capacitor provides energy to the load and output voltage continues to reduce in this period. The equivalent circuit in this stage is Fig. 8.

$Tr6$ turns off a little before t_2. The secondary current will charge snubber capacitor $C6$ and discharge snubber capacitor $C5$. During this very short transitional time, the secondary current flows through $D8$ to charge and discharge snubber capacitors. When $C5$ is totally discharged $(Vds5 = 0)$, the secondary current will flow through $D5/D8$ and the energy will be transferred to the load. The corresponding equivalent circuits are Fig. 9-Fig. 10.

3: Stage 3 $t_2 - t_3$: The control signal $Vg5/Vg8 = 1$, power switches $Tr5/Tr8$ will turn on at t_2. Because $I_{as} > 0$ during this stage, the secondary side current will flow through $Tr5/Tr8$ and transfer energy to the load in this stage. The output voltage will increase in this stage. The equivalent circuit in this stage is shown in Fig. 11.

4: Stage 4 $t_3 - t_4$: $Vg4/Vg8 = 0$, so, $Tr4/Tr8$ will turn off at t_3.

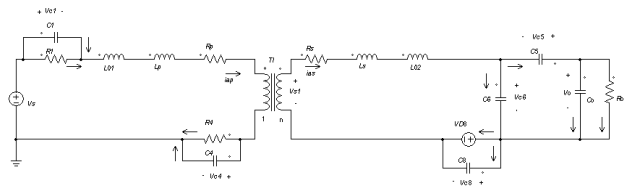

Fig. 9: Charge-Discharge Equivalent Circuit in Stage 2

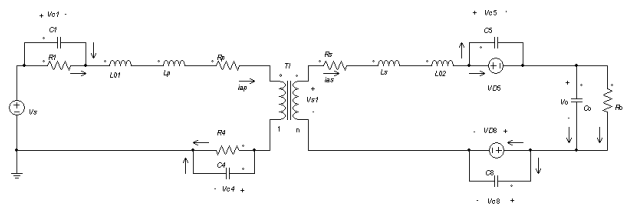

Fig. 10: Diode Conduct Equivalent Circuit in Stage 2

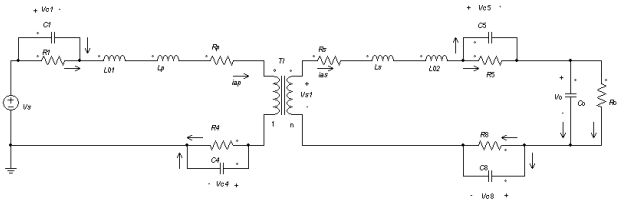

Fig. 11: Energy Transfer Equivalent Circuit in Stage 3

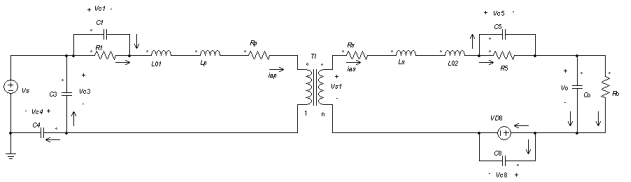

Fig. 12: C3 Discharge Equivalent Circuit in Stage 4

For the primary side, $Tr4$ turns off at t_3, The primary current will charge snubber capacitor $C4$ and discharge snubber capacitor $C3$. When $C3$ is totally discharged $(Vds3 = 0)$, the primary current will flow through $Tr1/D3$ and form a freewheeling period. No power is transferred to the secondary side theoretically.

For the secondary side, the current $I_{as} > 0$, this indicates $Tr5/D8$ will continue conduct in this period of time. The additional inductor $L02$ and secondary leakage inductance will provide energy to transfer to the load. The output voltage will continue to increase in this stage. The equivalent circuits are shown in Fig. 12 and Fig. 13.

$Tr1$ turns off a little before t_4. The primary current will discharge snubber capacitor $C2$ and charge snubber capacitor $C1$. During this very short transitional time, the current will flow through $D3$ to charge and discharge capacitors. When $C2$ is totally discharged $(Vds2 = 0)$, $D2$ will conduct and form an energy feedback to power source. This will make it feasible for $Tr2/Tr3$ to turn on under ZVS. The equivalent circuits are shown in Fig. 14 and Fig. 15.

5: Stage 5 $t_4 - t_5$: Because $Vg2/Vg3 = 1$, $Tr2/Tr3$ will turn on at t_4 under ZVS. Because the primary current $i_{ap} > 0$, the energy will feedback to the primary source in this interval.

For the secondary side, $Vg5 = 1$, so, $Tr5$ is On in this interval. $Vg6/Vg7/Vg8 = 0$, so, $Tr6/Tr7/Tr8$ will be in off state during this period of time. Because the secondary current $i_{as} > 0$, $Tr5/D8$ will conduct in this period of time. The inductor $L02$, the secondary

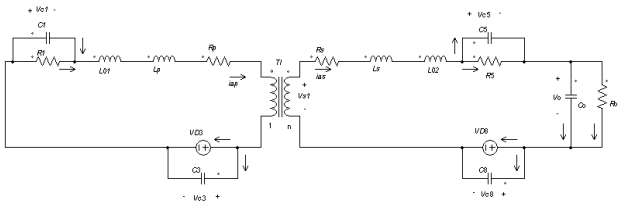

Fig. 13: Free Wheeling Equivalent Circuit in Stage 4

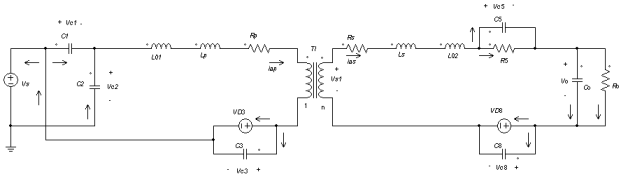

Fig. 14: C2 Discharge Equivalent Circuit in Stage 4

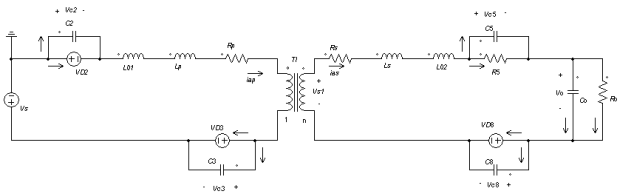

Fig. 15: Energy Feedback Equivalent Circuit in Stage 4

leakage inductor and output capacitor will provide energy to the load together in this interval. The output voltage begins to reduce in this interval. According to this analysis, the equivalent circuits in this interval can be got similarly.

6: Stage 6 $t_5 - t_6$: Because $Vg2/Vg3 = 1$, $Tr2/Tr3$ will be on in this stage. Because the primary current $I_{ap} < 0$, the energy will transfer to the secondary side again.

For the secondary side, $Vg5 = 1$, so, $Tr5$ is on state in this stage.$Vg6/Vg7/Vg8 = 0$, so, $Tr6/Tr7/Tr8$ all will be in off state during this period of time. Because the secondary side current $I_{as} < 0$, secondary current will charge capacitor $C8$ and discharge capacitor $C7$ till its voltage reduces to the forward conduction voltage of diode $D7$. Then the current flows through $Tr5/D7$ in this period of time and form a freewheeling period with no energy transferred to the load theoretically in this stage. The energy from primary source is stored in $L02$ and leakage inductor. Output capacitor provides energy to the load and output voltage will continue to reduce in this stage. The equivalent circuit can be got similarly in this stage.

7: Stage 7 $t_6 - t_7$: Because $Vg6/Vg7 = 1$, $Tr6/Tr7$ will turn on at t_6. $Vg5 = 0$, so $Tr5$ turns off a little before t_6. The secondary current will charge $C5$ and discharge $C6$. During this very short of transitional time, the secondary current flows through $D7$ to charge and discharge snubber capacitors. When $C6$ is totally discharged $(Vds6 = 0)$, $D6$ will turn on and $D6/D7$ will conduct to form ZVS and transfer energy to the load. Because the secondary side current $I_{as} < 0$, $Tr6/Tr7$ will conduct in this period of time and transfer energy to the load in this stage. The output voltage will increase in this stage. The equivalent circuits in this stage can be got similarly.

8: Stage 8 $t_7 - t_8$: Because $Vg3/Vg7 = 0$ at t_7, $Tr3/Tr7$ will turn off at t_7. For the primary side, $Tr3$ turns off; the primary current will charge $C3$ and discharge $C4$. During this very short of transitional time, the primary current flows through $Tr2$ to charge and discharge snubber capacitors $C3$ and $C4$. When $C4$ is totally discharged $(Vds4 = 0)$, $D4$ will turn on. $Tr2/D4$ conduct, this forms a freewheeling stage with no energy transferred to the secondary side theoretically.

Tr2 turns off a little before t_8. The energy stored in additional inductor $L01$ and transformer leakage inductance will charge the snubber capacitor $C2$ and discharge snubber capacitor $C1$. During this very short transitional time, the primary current flows through $D4$ to charge and discharge snubber capacitors. When $C1$ is discharged totally $(Vds1 = 0)$, then the primary current will flow through $D4/D1$ and the inductor energy flows back to the power source.

For the secondary side, $Tr6/D7$ will continue conduct during this period of time and transfer energy to the load. This is because the secondary side current $I_{as} < 0$. The energy mainly comes from the stored energy of additional inductor $L02$ and the leakage inductance. Output voltage will continue to increase in this stage. The corresponding equivalent circuits can be got similarly according to the analysis for this stage.

IV. Important Equations For Each Stage Of Forward Bidierctional Dual Full Bridge Converter With Novel Triple-Phase-Shift Control

Based on the equivalent circuits in each stage, the corresponding equivalent inductor voltage and output capacitor current equations can be built for this bidirectional DC-DC converter in each stage.

A. Necessary Equations in Stage 1 $(t_0 - t_1)$

The necessary equation of the converter can be built according to the equivalent circuit Fig.6 in this stage as following:

$$\begin{cases} (L01 + Lp + \frac{1}{n^2} * Ls)\frac{di_{ap}}{dt} = -\frac{1}{n} * Vo - Vs - \\ \qquad (Rp + R1 + R4 + \frac{1}{n^2} * Rs + \frac{1}{n^2} * R6) * i_{ap} \\ Co\frac{dvo}{dt} = \frac{1}{n} * i_{ap} - \frac{vo}{Ro} \end{cases} \tag{1}$$

B. Necessary Equations in Stage 2 $(t_1 - t_2)$

From the previous analysis of the converter working process, it can be found there are four sub-stages and corresponding four equivalent circuits in this stage.

(1) Sub-stage of Charge-discharge of $C7$ and $C8$
According to the equivalent circuit of the converter shown in Fig. 7, the equation can be built as following:

$$\begin{cases} (L01 + Lp + \frac{1}{n^2} * L02 + \frac{1}{n^2} * Ls)\frac{di_{ap}}{dt} = -(Rp + R1 + \\ \qquad R4 + \frac{1}{n^2} * Rs + \frac{1}{n^2} * R6) * iap - \frac{1}{n} * Vc7 + Vs \\ Co\frac{dvo}{dt} = -\frac{vo}{Ro} \end{cases} \tag{2}$$

(2) Sub-stage of Free Wheeling in Stage 2
According to the equivalent circuit of the converter in freewheeling stage shown in Fig. 8, the corresponding equation can be built as following:

$$\begin{cases} (L01 + Lp + \frac{1}{n^2} * L02 + \frac{1}{n^2} * Ls)\frac{di_{ap}}{dt} = -(Rp + R1 \\ \qquad +R4 + \frac{1}{n^2} * Rs + \frac{1}{n^2} * R6) * i_{ap} + Vs \\ Co\frac{dvo}{dt} = -\frac{vo}{Ro} \end{cases} \tag{3}$$

(3) Sub-stage of $C5/C6$ Charge and Discharge in Stage 2
According to the equivalent circuit of the converter in this stage shown in Fig. 9, the corresponding equation can be built as following:

$$\begin{cases} (L01 + Lp + \frac{1}{n^2} * L02 + \frac{1}{n^2} * Ls)\frac{di_{ap}}{dt} = -(Rp + R1 + \\ \qquad R4 + \frac{1}{n^2} * Rs + \frac{1}{n^2} * R6) * i_{ap} - \frac{1}{n} * Vc6 + Vs \\ Co\frac{dvo}{dt} = -\frac{vo}{Ro} \end{cases} \tag{4}$$

(4) Sub-stage of $D5/D8$ Conduction in Stage 2
According to the equivalent circuit of the converter in this stage shown in Fig. 10, the corresponding equation can be built as following:

$$\begin{cases} (L01+Lp+\frac{1}{n^2}*L02+\frac{1}{n^2}*Ls)\frac{di_{ap}}{dt} = -(Rp+R1+ \\ \qquad\qquad R4+\frac{1}{n^2}*Rs)*i_{ap}-\frac{1}{n}*Vo+Vs \\ Co\frac{dvo}{dt} = \frac{1}{n}*i_{ap}-\frac{vo}{Ro} \end{cases} \tag{5}$$

C. Necessary Equations in Stage 3 $(t_2 - t_3)$

The energy is transferred to the DC load in this stage. According to the equivalent circuit of the converter in this stage shown in Fig. 11, the corresponding equation can be built as following:

$$\begin{cases} (L01+Lp+\frac{1}{n^2}*L02+\frac{1}{n^2}*Ls)\frac{diap}{dt} = -(Rp+R1+ \\ \qquad\qquad R4+\frac{1}{n^2}*Rs+\frac{1}{n^2}*R5+\frac{1}{n^2}*R8)*iap \\ \qquad\qquad -\frac{1}{n}*Vo+Vs \\ Co\frac{dvo}{dt} = \frac{1}{n}*iap-\frac{vo}{Ro} \end{cases} \tag{6}$$

D. Necessary Equations in Stage 4 $(t_3 - t_4)$

From the previous analysis of the converter working process, it can be found there are four sub-stages in this stage. The first two main sub-stages are analyzed here. The necessary equations can be built as following:

(1) Sub-stage of $C3/C4$ Charge and Discharge in Stage 4
According to the equivalent circuit of the converter in this stage shown in Fig. 12, the corresponding equation can be built as following:

$$\begin{cases} (L01+Lp+\frac{1}{n^2}*L02+\frac{1}{n^2}*Ls)\frac{di_{ap}}{dt} = -(Rp+R1+ \\ \qquad\qquad R4+\frac{1}{n^2}*Rs+\frac{1}{n^2}*R5+\frac{1}{n^2}*R8)*iap \\ \qquad\qquad -\frac{1}{n}*Vo+Vs \\ Co\frac{dvo}{dt} = \frac{1}{n}*iap-\frac{vo}{Ro} \end{cases} \tag{7}$$

$$\begin{cases} (L01+Lp+\frac{1}{n^2}*L02+\frac{1}{n^2}*Ls)\frac{di_{ap}}{dt} = -(Rp+R1+ \\ \qquad\qquad \frac{1}{n^2}*Rs+\frac{1}{n^2}*R5)*i_{ap}-Vc4-\frac{1}{n}*Vo+Vs \\ Co\frac{dvo}{dt} = \frac{1}{n}*i_{ap}-\frac{vo}{Ro} \end{cases} \tag{8}$$

(2) Sub-stage of $Tr1/D3$ Conduction in Stage 4
This is another freewheeling sub-stage in primary power circuit; according to the equivalent circuit Fig. 13, the necessary equations can be built as following:

$$\begin{cases} (L01+Lp+\frac{1}{n^2}*L02+\frac{1}{n^2}*Ls)\frac{di_{ap}}{dt} = -(Rp+R1+ \\ \qquad\qquad \frac{1}{n^2}*Rs+\frac{1}{n^2}*R5)*i_{ap}-\frac{1}{n}*Vo \\ Co\frac{dvo}{dt} = \frac{1}{n}*i_{ap}-\frac{vo}{Ro} \end{cases} \tag{9}$$

The necessary equations for other two very short sub-stages in this stage and left four stages can be built similarly according to the working process analysis.

V. Voltage Ratio, Active Power And Efficiency Of Forward Bidirectional Dual Full Bridge Converter With Novel Triple-Phase-Shift Control

It is well known that the converter loss mainly includes conduction loss and switching loss [10], [15]. The switching loss of the converter is eliminated because this converter can realize ZVS very well in large load scope. In the following power and efficiency expressions, only the conduction loss of power MOSFETs and the loss of the winding resistance of the transformer are considered.

A. The Expression of Voltage Ratio Vo/Vs

In order to be convenient to see clearly the major role of triple phase-shift control method, the power MOSFETs and diodes are treated as ideal. The winding resistance of the transformer is neglected. From the working process analysis and the simulation waveforms shown in Fig. 5, it can be found the inductor current iap crosses zero half period of Ts. The first stage $(t_0 - t_1)$ and the fifth stage $(t_4 - t_5)$ are due to the dead band effect. They are neglected here. In order to be convenient, write:

$$L_{eq} = L01+Lp+\frac{1}{n^2}*L02+\frac{1}{n^2}*Ls \tag{10}$$

Because the time interval of snubber capacitors charge/discharge is very short compared with the stage time duration, it can be neglected, too. From Fig. 5, it can be found the corresponding stages are equal to:

$$\begin{cases} t2-t0 = D1*Ts \\ t3-t2 = (0.5-D3)*Ts \\ t4-t3 = D2*Ts \end{cases} \tag{11}$$

Apply Volt-second balance and small ripple approximation to equivalent inductor L_{eq}, there is:

$$Vs*D1+(-\frac{vo}{n}+Vs)*(0.5-D3)+(-\frac{vo}{n})*D2 = 0 \tag{12}$$

The output voltage can be got from this equation as following:

$$\frac{vo}{vs} = \frac{n*(1+2D1-2D3)}{(1+2D2-2D3)} \tag{13}$$

This formula suggests that the output voltage depends on three control variables. This will make the output voltage more robust to parameter changes. With novel triple-phase-shift control, the output voltage behaves very well when the first reference voltage is equal to $5/6/7/8Volts$ or other values in the control circuit. With dual or single phase-shift control, the average output voltage will be always equal to zero when the first reference voltage in the control circuit is equal to or higher than $6Volts$, Fig. 16 and Fig. 17.

B. The Expression of Primary Current in First Half Period

According to the primary current differential equation listed in section IV, there are three main current expressions in the first half period. The current expressions in ZVS sub-stages need not to be considered because the time for ZVS sub-stages are very short and there is no active power in ZVS sub-stages theoretically.
(1)The Expression of Primary Current in Stage $t_0 - t_2$ Write:

$$Req1 = Rp+R1+R4+\frac{1}{n^2}*Rs+\frac{1}{n^2}*R6 \tag{14}$$

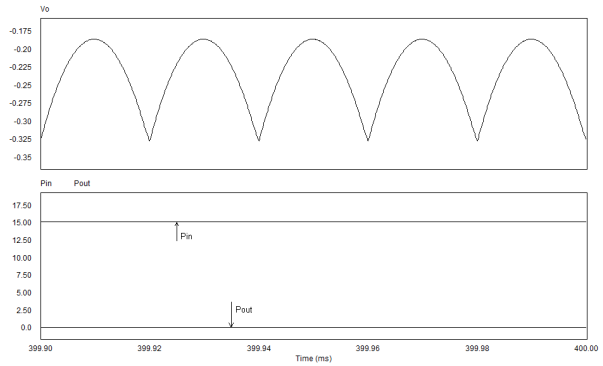

Fig. 16: Forward Simulation Results with Dual Phase-shift Control When Vref1¿=6V

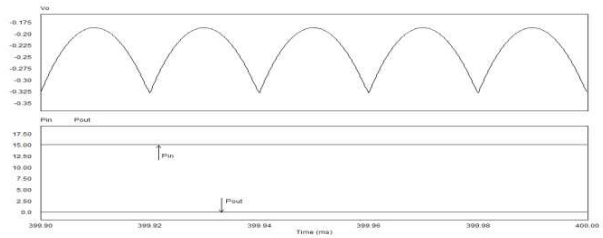

Fig. 17: Forward Simulation Results with Single Phase-shift Control When Vref1¿=6V

Primary current in this stage can be solved out as:

$$i_{ap} = \frac{vs}{Req1} * (1 - e^{\frac{-Req1*t}{Leq}}) \tag{15}$$

(2)The Expression of Primary Current in Stage $t_2 - t_3$ Write:

$$Req2 = Rp + R1 + R4 + \frac{1}{n^2} * Rs + \frac{1}{n^2} * R5 + \frac{1}{n^2} * R8 \tag{16}$$

Primary current in this stage can be solved out as:

$$\begin{cases} i_{ap}(t2+) = iap(t2-) = \frac{vs}{Req1} * (1 - e^{\frac{-Req1*D1*TS}{Leq}}) \\ i_{ap} = \frac{vs - \frac{vo}{n}}{Req2} + [i_{ap}(t2+) - \frac{vs - \frac{vo}{n}}{Req2}] * e^{\frac{-Req2*t}{Leq}} \end{cases} \tag{17}$$

(3)The Expression of Primary Current in Stage $t_3 - t_4$ Write:

$$Req3 = Rp + R1 + \frac{1}{n^2} * Rs + \frac{1}{n^2} * R5 \tag{18}$$

Primary current in this stage can be solved out as:

$$\begin{cases} i_{ap}(t3+) = i_{ap}(t3-) = i_{ap}(t3-) = \frac{vs - \frac{vo}{n}}{Req2} + [i_{ap}(t2+) \\ \qquad - \frac{vs - \frac{vo}{n}}{Req2}] * e^{\frac{-Req2*(0.5-D2)*TS}{Leq}} \\ i_{ap} = \frac{-vo}{n*Req3} + [i_{ap}(t3+) + \frac{vo}{n*Req3}] * e^{\frac{-Req3*t}{Leq}} \end{cases} \tag{19}$$

The primary current expressions in the second half period are equal to the negative of the corresponding expressions listed above.

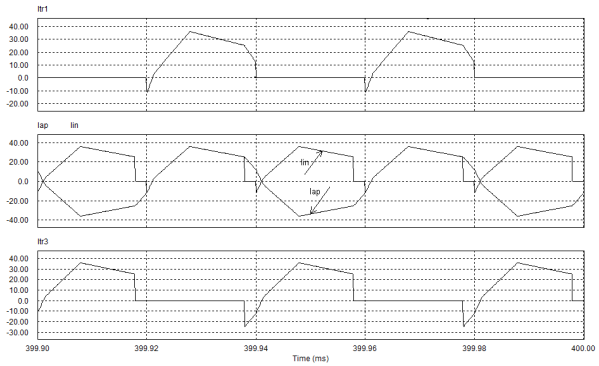

Fig. 18: Forward Simulation Waveforms of Input Current, Primary Current and Power Switch Currents

C. The Expression of Average Input Power

From the working process of the bidirectional converter and the above simulation results Fig. 18, it can be found the primary power circuit does not transfer power to the secondary side during the freewheeling stage $(t_3 - t_4)$ in the first half working period, the situation is similar in the second half working period. Therefore, the average input active power is equal to:

$$Pin = \frac{2}{Ts} \int_0^{\frac{Ts}{2}} Vs * i_{in}\, dt = \frac{2vs}{Ts} \int_0^{\frac{Ts}{2}} i_{ap}\, dt \tag{20}$$

Substituting the corresponding expressions of iap into above equation, the average input active power can be got as following:

$$\begin{aligned} Pin = \frac{2 * Vs^2}{Ts} * Y_2 = \frac{2 * Vs^2}{Ts} * [& \frac{D1 * Ts}{Req1} + \frac{Leq}{Req1^2} \\ & * e^{\frac{-Req1*D1*tS}{Leq}} - \frac{Leq}{Req1^2} + \frac{Ts}{Req2} \\ & * \frac{(D2 - D1) * (1 - 2 * D2)}{(1 + 2 * D2 - 2 * D3)} \\ & - \frac{2 * D1 * (D2 - D1) * Ts}{(1 + 2 * D2 - 2 * D3) * Req2} \\ & - \frac{Leq}{Req1 * Req2} * (1 - e^{\frac{Req1*D1*Ts}{Leq}}) \\ & * e^{\frac{-Req2*(0.5-D2)*Ts}{Leq}} + \frac{Leq}{Req1 * Req2} \\ & * (1 - e^{\frac{-Req1*D1*Ts}{Leq}}) * e^{\frac{-Req2*D1*Ts}{Leq}}] + \frac{2 * vs^2}{Ts} \\ * [& \frac{2 * Leq * (D2 - D1)}{(1 + 2 * D2 - 2 * D3) * rEQ2^2} * e^{\frac{-Req2*(0.5-D2)*Ts}{Leq}} \\ & * [\frac{2 * Leq * (D2 - D1)}{(1 + 2 * D2 - 2 * D3) * rEQ2^2} * e^{\frac{-Req2*D1*Ts}{Leq}} \end{aligned} \tag{21}$$

It can be found the average input active power is decided by three phase-shifts, working period Ts, power switch conduction loss, equivalent inductance and winding resistance of the transformer.

D. The Expression of Average output Power

From the working process of the bidirectional converter and the above simulation results Fig. 19, it can be found the secondary power circuit does not transfer power to the load during the freewheeling stage $(t_0 - t_2)$ in the first half working period, the situation is similar in the second half working period. Therefore, the average output active power is equal to:

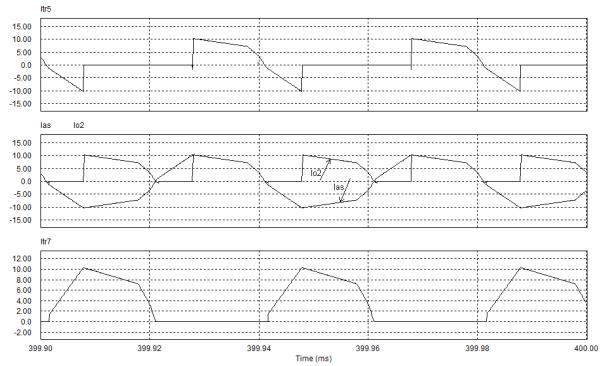

Fig. 19: Forward Simulation Waveforms of Output Current, Secondary Current and Power Switch Currents

$$Pout = \frac{2}{Ts}\int_0^{\frac{Ts}{2}} Vo * i_o\, dt = \frac{2vo}{nTs}\frac{2vs}{Ts}\int_0^{\frac{Ts}{2}} i_{ap}\, dt \tag{22}$$

Substituting the corresponding expressions of iap into above equation, the average output power can be got.

$$\begin{aligned}
Pout = {} & \frac{2 * vs^2 * (1 + 2 * D1 - 2 * D3)}{Ts * (1 + 2 * D2 - 2 * D3)} * Y1 \\
Y1 = {} & [\frac{(D2 - D1) * (1 - 2 * D2) * Ts}{(1 + 2 * D2 - 2 * D3) * Req2} \\
& - \frac{2 * D1 * (D2 - D1)}{(1 + 2 * D2 - 2 * D3) * Req2} \\
& - \frac{Leq}{Req1 * Req2} * (1 - e^{\frac{Req1 * D1 * Ts}{Leq}}) \\
& * e^{\frac{-Req2 * (0.5 - D2) * Ts}{Leq}} \\
& + \frac{Leq}{Req1 * Req2} * (1 - e^{\frac{Req1 * D1 * Ts}{Leq}}) \\
& * e^{\frac{-Req2 * D1 * Ts}{Leq}} \\
& + \frac{2 * (D2 - D1) * Leq}{(1 + 2 * D2 - 2 * D3) * Req2^2} \\
& * e^{\frac{-Req2 * (0.5 - D2) * Ts}{Leq}} \\
& - \frac{2 * (D2 - D1) * Leq}{(1 + 2 * D2 - 2 * D3) * Req2^2} \\
& * e^{\frac{-Req2 * D1 * Ts}{Leq}} \\
& - \frac{(1 + 2 * D1 - 2 * D3) * Ts}{2 * (1 + 2 * D2 - 2 * D3) * Req3} \\
& + \frac{(1 + 2 * D1 - 2 * D3) * (0.5 - D2) * Ts}{2 * (1 + 2 * D2 - 2 * D3) * Req3} \\
& - \frac{2 * (D2 - D1) * Leq}{(1 + 2 * D2 - 2 * D3) * Req2 * Req3} \\
& * e^{\frac{-Req3 * Ts}{2 * Leq}} \\
& + \frac{2 * (D2 - D1) * Leq}{(1 + 2 * D2 - 2 * D3) * Req2 * Req3} \\
& * e^{\frac{-Req3 * (0.5 - D2) * Ts}{Leq}} \\
& - \frac{Leq}{Req1 * Req3} \\
& * e^{\frac{-Req2 * (0.5 - D2) * Ts - 0.5 * Req3 * Ts}{Leq}} \\
& + \frac{Leq}{Req1 * Req3} \\
& * e^{\frac{-Req1 * D1 * Ts - Req2 * (0.5 - D2) * Ts - 0.5 * Req3 * Ts}{Leq}} \\
& + \frac{2 * (D2 - D1) * Leq}{(1 + 2 * D2 - 2 * D3) * Req2 * Req3} \\
& * e^{\frac{-Req3 * (0.5 - D2) * Ts - 0.5 * Req3 * Ts}{Leq}} \\
& + \frac{Leq}{Req1 * Req3} * e^{\frac{-Req2 * (0.5 - D2) * Ts - 0.5 * Req3 * Ts}{Leq}} \\
& - \frac{Leq}{Req1 * Req3} \\
& * e^{\frac{-Req1 * D1 * Ts - Req2 * (0.5 - D2) * Ts - 0.5 * Req3 * Ts}{Leq}} \\
& + \frac{2 * (D2 - D1) * Leq}{(1 + 2 * D2 - 2 * D3) * Req2 * Req3} \\
& * e^{\frac{-Req2 * (0.5 - D2) * Ts - 0.5 * Req3 * Ts}{Leq}} \\
& + \frac{Leq}{Req1 * Req3} \\
& * e^{\frac{-Req2 * (0.5 - D2) * Ts - Req3 * (0.5 - D2) * Ts}{Leq}} \\
& - \frac{Leq}{Req1 * Req3} \\
& * e^{\frac{-Req1 * D1 * Ts - Req2 * (0.5 - D2) * Ts - (0.5 - D2) * Req3 * Ts}{Leq}} \\
& - \frac{Leq * (1 + 2 * D1 - 2 * D3)}{Req3^2 * (1 + 2 * D2 - 2 * D3)} * e^{\frac{Req3 * Ts}{2 * Leq}} \\
& + \frac{Leq * (1 + 2 * D1 - 2 * D3)}{Req3^2 * (1 + 2 * D2 - 2 * D3)} \\
& * e^{\frac{Req3 * (0.5 - D2) * Ts}{Leq}}]
\end{aligned} \tag{23}$$

It can be found the average output active power is decided by three phase-shifts, working period Ts, power switch conduction loss, equivalent inductance and winding resistance of the transformer, too.

E. The Efficiency of the Bidirectional Converter

$$\eta = \frac{Pout}{Pin} \tag{24}$$

Substitute the expressions of average input power and average output power into the above equation, the efficiency of this bidirectional converter with triple phase-shift control method can be solved out as follows:

$$\eta = \frac{(1 + 2 * D1 - 2 * D3) * Y1}{(1 + 2 * D2 - 2 * D3) * Y2} \tag{25}$$

It can be found clearly that the efficiency of the bidirectional converter with novel triple-phase-shift control mainly depends on three control variables. This will make it more robust to parameter and output power change.

From the simulation waveforms and efficiency comparison data listed in Tab. II, it can be seen clearly the novel triple phase-shift control is much better than other two control methods when magnetizing inductance Lm changes with an unknown rule during the simulation process. This suggests the novel triple phase control will make the efficiency of the bidirectional converter much more robust (insensitive) to parameter change than other existing control methods.

In order to check whether this novel triple phase-shift control method can make the bidirectional converter with high efficiency in large load scope, this bidirectional ZVS DC-DC converter with novel triple-phase-shift control is simulated with PSIM software for four different output powers. The corresponding efficiency is listed

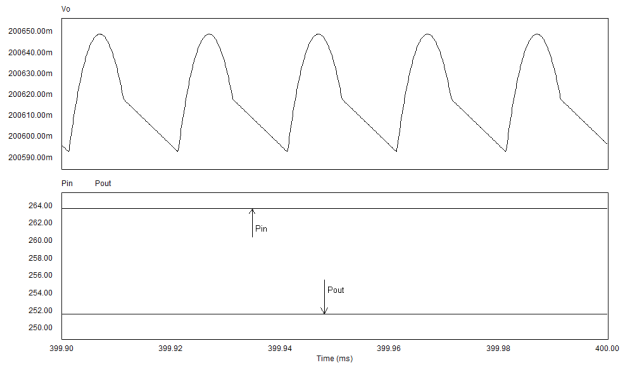

Fig. 20: Simulation Results of Forward Converter with novel Triple-Phase-shift Control (L01=L02=0, Pout=250W)

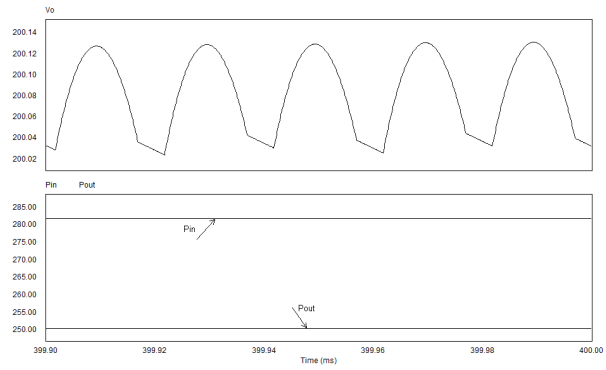

Fig. 21: Simulation Results of Forward Converter with Dual Phase-shift Control (L01=L02=0, Pout=250W)

as following.

VI. Simulation Studies And Discussio

When parameter and output power change, the simulation waveforms and efficiency of the bidirectional converter with three different control methods is attached in the following. They are simulated with PSIM software shown in Fig. 20, Fig. 21 and Fig. 22.

The following table gives the efficiency comparison of the bidirectional dual full bridge converter with three different control methods when parameter and output power change.

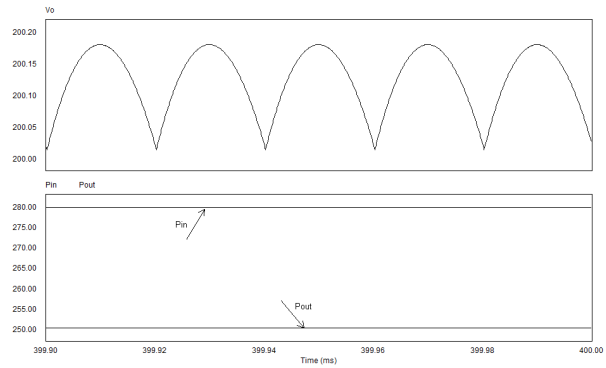

Fig. 22: Simulation Results of Forward Converter with Single Phase-shift Control (L01=L02=0, Pout=250W)

TABLE I: Forward Efficiency Comparison When Parameter Changes ($L01 = L02 = 0$)

Output Power	Single Phase-shift	Dual Phase-shift	Novel Triple Phase-shift
$1kW$	95.4%	95.6%	96.7%
$250W$	89.4%	88.8%	95.4%

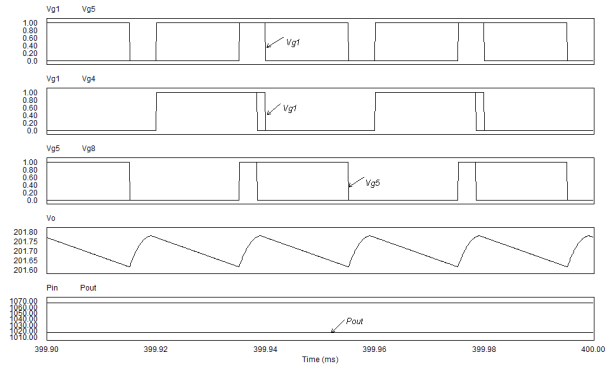

Fig. 23: Simulation Results of Forward Converter with Triple Phase-shift Control When Lm Changes Randomly

TABLE II: Converter Efficiency Comparison When Magnetizing Inductance Lm Changes Randomly

Output Power	Single Phase-shift	Dual Phase-shift	Novel Triple Phase-shift
Forward $1kW$	85%	85.5%	95.3%
Backward $250W$	70.2%	92.5%	96.5%

From these simulation waveforms and the efficiency data listed in Tab. I, it can be found the efficiency of bidirectional power circuit with novel triple phase-shift control is better than the efficiency of the same bidirectional power circuit with other control methods when serial inductance $L01$ changes from $7.3uH$ to $zero$, serial inductance $L02$ changes from $6.9uH$ to $zero$ or output power changes from $1kW$ to $250W$.

If a certain value is not assumed to magnetizing inductance Lm of the transformer, it will change with an unknown rule during the process of simulation with PSIM. This will make the simulation results nearly the same as the real application situation. The forward simulation waveforms of these three control methods with the same bidirectional dual full bridge ZVS converter are attached in Fig. 23, Fig. 24 and Fig. 25.

From the simulation waveforms and efficiency comparison data listed in Tab. II, it can be seen clearly the novel triple phase-shift control is much better than other two control methods when

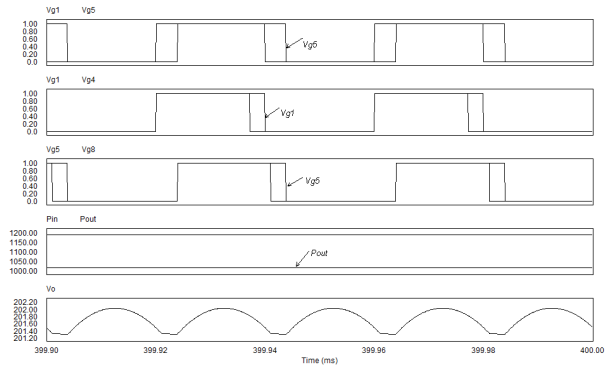

Fig. 24: Simulation Results of Forward Converter with Dual Phase-shift Control When Lm Changes Randomly

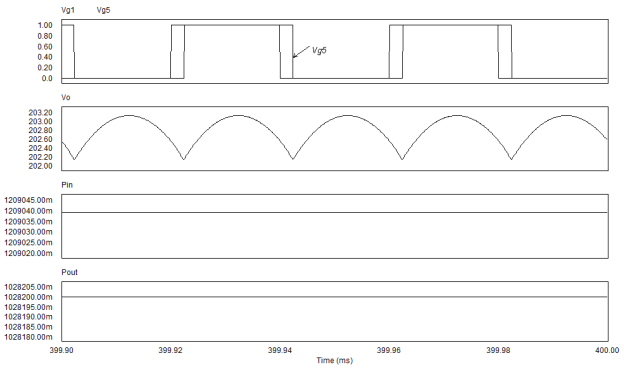

Fig. 25: Simulation Results of Forward Converter with Single Phase-shift Control When Lm Changes Randomly

TABLE III: Forward Output Power and Efficiency

Pout(W)	1003.00	754.75	502.50	252.53
Efficiency	97.6%	97.6%	98.4%	98.5%
Vo(V)	200.30 ±0.019%	200.57 ±0.015%	200.54 ±0.01%	201.01 ±0.006%

TABLE IV: Backward Output Power and Efficiency

Pout(W)	1008.32	751.88	499.84	250.53
Efficiency	96.9%	97.3%	98.0%	98.4%
Vo(V)	48.16 ±0.025%	48.04 ±0.019%	47.95 ±0.015%	48.01 ±0.08%

magnetizing inductance Lm changes with an unknown rule during the simulation process. This suggests the novel triple phase control will make the efficiency of the bidirectional converter much more robust (insensitive) to parameter change than other existing control methods.

In order to check whether this novel triple phase-shift control method can make the bidirectional converter with high efficiency in large load scope, this bidirectional ZVS DC-DC converter with novel triple-phase-shift control is simulated with PSIM software for four different output powers. The corresponding efficiency is listed as Tab. III-Tab. IV.

VII. Conclusion

This paper analyzes the working theory of a bidirectional dual full bridge ZVS DC-DC converter with novel triple phase-shift control method in detail. It separates the nonlinear converter into several linear stages in one period; find its equivalent circuits and build corresponding necessary equations for each stage. The forward output voltage and input voltage ratio, average input active power, average output active power and efficiency are solved theoretically. Relevant simulation demonstrations for this method are provided in this paper.

The simulation results demonstrate that this novel control method makes the efficiency and output voltage of this bidirectional converter more robust (insensitive) to parameter and output power change. Simulation results also show that the forward and backward efficiency of this bidirectional converter for four different output powers are very satisfactory. This suggests this novel triple-phase-shift control method can make the converter realize ZVS and work well in large load scope.

References

[1] L. Zhu, "A novel soft-commutating isolated boost full bridge ZVS-PWM dc-dc converter for bidirectional high power applications," *IEEE Trans. Power Electronics,* vol. 21, No.2, pp. 422-429, March, 2006.

[2] H.J. Chiu and L.W. Lin, "A bidirectional DC-DC converter for fuel cell electric vehicle driving systems," *IEEE Trans. Power Electronics,* vol. 21, no. 4, pp. 950-958, July. 2006.

[3] Shigenori Inoue and Hirofumi Akagi, "A Bidirectional DC-DC Converter for an Energy Storage System with Galvanic Isolation," *IEEE Trans. Power Electronics,* vol. 22, no. 6, Nov. 2007.

[4] Hua Bai and Chris Mi, "Eliminate Reactive Power and Increase System Efficiency of Isolated Bidirectional Dual Active Bridge DC-DC Converters Using Novel Dual Phase Shift Control," *IEEE Trans. Power Electronics,* vol .23, no. 6, Nov. 2008.

[5] Robert W. Erickson, Dragan Maksimovic, "Fundamentals of Power Electronics (Second Edition)," *Springer Science +Business Media,* Inc. 2001.

[6] Gr2aham C. Goodwin , Stefan F. Graebe, Mario E. Salgado , "Control System Design," *Prentice Hall of India,* 2006.

[7] C.W. de Silva, "Modeling and Control of Engineering Systems," *Boca Raton,* FL: CRC Press, 2009.

[8] Y. Hu, J. Tatler and Z. Chen, "A bidirectional dc/dc power electronic converter for an energy storage device in an autonomous power system," *Proc. Power Electronics. Motion Cont. Conf. (IPMEC),* vol. 1. pp. 171-176, 2004.

[9] D.H.Xu, C.H. Zhao and H. F. Fan, "A PWM plus phase-shift control bidirectional DC-DC converter," *IEEE Trans.Power Electronics,* vol. 19, no. 3, pp. 666-675, May. 2004.

[10] Z. Ye, P. Jain, and P. Sen, "Circulating current minimization in high frequency AC power distribution architectures with multiple inverter modules operated in parallel," *IEEE Trans. Industrial Electronics,* vol. 54, no. 5, pp. 2673-2687, Oct. 2007

[11] Kuiyuan Wu and William G. Dunford, "An Unusual Full Bridge Converter to Realize ZVS in Large Load Scope," *Asian Power Electronics Journal,* vol. 2, no. 1, pp. 66-71, Apr, 2008.

[12] K. Lo, Y. Lin, T. Hsieh, "Phase-Shifted Full-Bridge Series-Resonant DC-DC Converters for Wide Load Variations," *IEEE Trans. Industrial Electronics,* pp. 1, 2011.

[13] Jianming Hu, Yuanrui Chen, Zijuan Yang, "Study and Simulation of One Bidirectional DC-DC Converter in Hybrid Electric Vehicle," *Proceedings of Third International Conference on Power Electronics Systems and Applications,* 2009.

[14] R.S. Yang, L.K. Chang, H.C. Chen, "An Isolated Full-Bridge DC-DC Converter with 1MHz Bidirectional Communication Channel," *IEEE Trans. Industrial Electronics,* pp. 1, 2011.

[15] S. Inoue and H. Akagi, "Loss Analysis of a bidirectional isolated dc/dc converter," *Proc. Int. Power Electronics Conf. (IPEC),* 2005.

[16] R. J. Wai, C.Y. Lin, J. J. Liaw, Y. R. Chang, "Newly-Designed ZVS Multi-Input Converter," *IEEE Trans. Industrial Electronics,* pp. 1, 2011.

[17] H. Ribeiro, B. Borges, "New Optimized Full-Bridge, Single Stage AC/DC Converters," *IEEE Trans. Industrial Electronics,* pp. 1, 2011.

[18] B. R. Lin, J. Y. Dong, J. J. Chen, "Analysis and Implementation of a ZVS/ZCS DC-DC Switching Converter with Voltage Step-Up," *IEEE Trans. Industrial Electronics,* pp. 1, 2011.